S. T. Wlodek[1]*
Department of Chemistry
University of Houston
Houston, TX 77204-5641, USA

J. Antosiewicz[†]
J. A. McCammon
Department of Chemistry and Biochemistry and Department of Pharmacology
University of California at San Diego
La Jolla, CA 92093-0365, USA

T. P. Straatsma
Environmental Molecular Sciences Laboratory
Pacific Northwest Laboratories
Richland, WA 99352

M. K. Gilson
Center for Advanced Research in Biotechnology
Rockville, MD 20850-3479, USA

J. M. Briggs
Department of Chemistry and Biochemistry and Department of Pharmacology
University of California at San Diego
La Jolla, CA 92093-0365, USA

Binding of Tacrine and 6-Chlorotacrine by Acetylcholinesterase

C. Humblet
Parke-Davis Pharmaceutical Research
Warner-Lambert Co.
Ann Arbor, MI 48105, USA

J. L. Sussman
Department of Structural Biology
The Weizmann Institute of Science
Rehovot 76100, Israel

Multiconfiguration thermodynamic integration was used to determine the relative binding strength of tacrine and 6-chlorotacrine by Torpedo californica *acetylcholinesterase. 6-Chlorotacrine appears to be bound stronger by 0.7 ± 0.4 kcal/mol than unsubstituted tacrine when the active site triad residue His-440 is deprotonated. This result is in excellent agreement with experimental inhibition data on electric eel acetylcholinesterase. Electrostatic Poisson–Boltzmann calculations confirm that order of binding strength, resulting in* ΔG *of binding of* −2.9

Received January 30, 1995; accepted May 12, 1995.

* To whom correspondence should be addressed.

† On leave from University of Warsaw, Warsaw 02-089, Poland.

Biopolymers, Vol. 38, 109–117 (1996)

CCC 0006-3525/96/010109-09

and −3.3 kcal/mol for tacrine and chlorotacrine, respectively, and suggest inhibitor binding does not occur when His-440 is charged. Our results suggest that electron density redistribution upon tacrine chlorination is mainly responsible for the increased attraction potential between protonated inhibitor molecule and adjacent aromatic groups of Phe-330 and Trp-84. © *1996 John Wiley & Sons, Inc.*

INTRODUCTION

Clinical studies show that cholinesterase inhibitors demonstrate some efficacy in the treatment of Alzheimer's disease patients.[1,2] One class of the most promising compounds that inhibit acetylcholinesterase (AChE) are acridine derivatives.[3,4] Recently, new experimental data on AChE inhibition activity of a few tacrine (THA) analogues have been obtained.[5] The highest inhibitory effect was observed for chloro substituted THA at position 6 (9-amino-6-chloro-1,2,3,4-tetrahydroacridine (Scheme 1), further referred to as ClTHA), which shows about 3- and 19-fold decrease of the IC_{50} factor with respect to unsubstituted THA for electric eel and human red blood cell AChE, respectively.[5]

In this paper we suggest an explanation of the above experimental data using both the multiconfiguration thermodynamic integration (MCTI) simulation technique,[6] and electrostatic calculations based on the Poisson–Boltzmann equation.[7]

METHODS

The following methodology is adopted here:

1. The model of AChE–THA is constructed based on the x-ray structure of the complex and an ab initio optimized tacrine geometry.
2. The most likely ionization states of the AChE–THA complex are determined at the conditions matching the inhibition experiments.
3. Thermodynamic integration simulation and electrostatic Poisson–Boltzmann calculations are performed to determine the relative binding strength of THA and ClTHA in the active site of AChE.

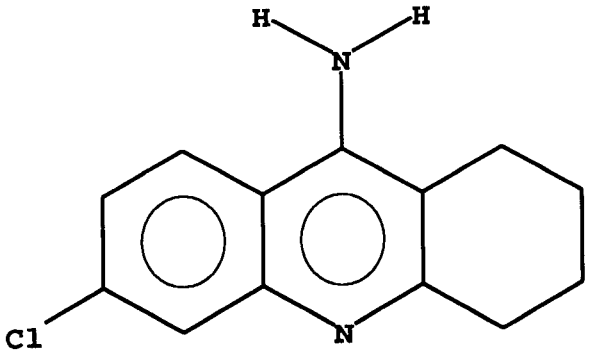

SCHEME I

Our calculations are based on the crystal structure of *Torpedo californica* AChE (TcAChE) liganded with the THA inhibitor.[8] All missing residues from the original protein data bank file (1–3, 486–489, 536, and 537) were reconstructed and energy minimized with the InsightII software (version 2.3.0; Biosym Technologies, San Diego, CA) using the CVFF force field. For the inhibitors, we used ab initio optimized structures. The relatively high basicity of tacrine (pKa 9.8[9]) indicates that at pH 7 this compound is completely protonated; therefore we performed geometry optimizations for protonated THA and ClTHA. All ab initio calculations were performed with the Gaussian 92 series of programs[10] and the 6-31G** basis set. Atomic charges were assigned with the CHELPG[11] procedure. Ab initio optimized THA or its N-ring protonated form was placed in the active site of TcAChE, rotated, and translated to fit the position and orientation provided in the crystal structure. The dimeric TcAChE–THA complex was then generated by symmetry inversion in such a way that a disulfide bond between SG atoms of terminal Cys-537 residues was formed.

Titration Calculations

The determination of the most likely ionization state of the complex was done with a numerical titration procedure developed in our group by Antosiewicz et al.[12] To describe this method briefly: self energies of all protein ionizable groups and interaction energies between them are calculated by solution of the linearized Poisson–Boltzmann equation for each group in the protein environment and in water, with the use of the UHBD program.[13] Those energies are used to calculate the mean charges and pKas of all ionizable groups with a Monte Carlo procedure[14] that samples the space of all possible ionization states, or with a so-called cluster method.[15] Protein atomic charges were taken from the CHARMm 22.0[16] set, which includes only polar hydrogen atoms, while for THA and ClTHA inhibitors atomic charges derived from the above mentioned quantum chemical calculations were used. Atomic radii were set to 0.5σ, where σ is the usual nonbonded parameter taken from the OPLS parameter set.[17] Atomic charges and radii for THA and

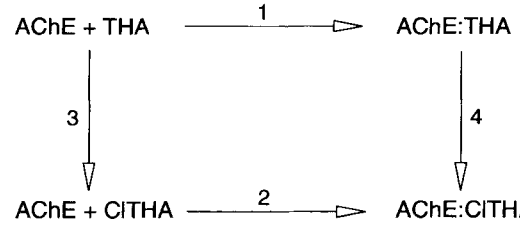

FIGURE 1 Thermodynamic cycle used in the calculation of $\Delta\Delta G$ for reactions 1 and 2. $\Delta\Delta G = \Delta G_4 - \Delta G_3$.

ClTHA molecules are shown in the Appendix. Protonation sites of histidine residues were adopted from a recent paper of Gilson et al.[18] In our titration calculations we used dielectric constants of 78 for the solvent and 20 for the protein. The reason for using such a high value for the protein dielectric constant is that it yields better agreement with measured pKas for a wide range of different proteins than lower values such as 4.[12] Both nitrogen atoms in the THA molecule were treated as ionizable sites, with initial pKas of 9.8 for the ring nitrogen[9] and 4.0 for the amino group (based on the low pKa value for aniline). Titration calculations were performed at the ionic strength matching the conditions of experimental inhibition study[5] performed in 50 m M phosphate buffer at pH 7. In order to reduce the computer time, only the monomeric enzyme was considered. We simply assumed that dimerization does not change the acid–base equilibria of the 143 ionizable residues in the monomer. This assumption recently gained support from electrostatic and Brownian dynamics simulations of AChE–substrate encounter kinetics[19] performed in our group, where no significant interaction between the enzyme subunits at physiological ionic strength was detected.

Thermodynamic Integration

The calculation of the free energy change, $\Delta\Delta G = \Delta G_2 - \Delta G_1$, for reactions 1 and 2 was based on the thermodynamic cycle shown in Figure 1. Processes 3 and 4 are nonphysical transformations of THA into ClTHA in water and in the active site of TcAChE, respectively. They can be simulated more easily than the real association reactions 1 and 2, which may involve large conformational changes of the enzyme. We have used the MCTI[6] for evaluation of the ΔG_3 and ΔG_4 values. In this technique, the free energy difference ΔG between two states of the system is approximated by a sum over ensemble averages for $\partial H/\partial\lambda$:

$$\Delta G = \int_0^1 \left(\frac{\partial H}{\partial \lambda}\right)_{\lambda_i} d\lambda \simeq \sum_i \left(\frac{\partial H}{\partial \lambda}\right)_{\lambda_i} \Delta\lambda \qquad (1)$$

where λ is a perturbation parameter, $0 \leq \lambda \leq 1$, coupling both states in such a way that its integer values 0 and 1 select the Hamiltonian H for those states.[6]

All MCTI simulations were done with the program ARGOS,[20] with the use of the OPLS/AMBER[17,21,22] force field with explicit aromatic hydrogen atoms for all Phe, Tyr, and Trp residues. We decided to use an all-atom representation for these aromatic rings because of the proximity of the THA inhibitor to two aromatic side chains in the active site of TcAChE (see next section). The ring nitrogen atom of THA does not belong to any atom types in the AMBER force field. We assumed, therefore, that it can be described by the same force constants that are used for aromatic carbon atoms. In the case of the tacrine amino group, we adopted AMBER parameters which are used to describe the sp^2 nitrogen in planar NH_2 groups. The results of our ab initio calculations given in the section on ligand and TcAChE–THA complex structures justify that choice.

Preliminary energy minimization of the TcAChE–THA system showed that the OPLS/AMBER force field strongly overestimates the intramolecular attraction between polar atoms 1–5 in the sequence 1-2-3-4-5 where atom 1 is a heavy atom and atom 5 is hydrogen. In the case of TcAChE the problem was manifested by the formation of an unusual 5-membered ring structure for Thr-126. That kind of behavior was seen before by Smith et al.[23] and recently by T. J. Marrone (personal communication, 1995). In order to fix the problem, we have replaced the original factor of $\frac{1}{8}$, which scales the Lennard–Jones parameters for so-called (1, 4) polar interactions, with a factor of $\frac{1}{2}$.

The protocol of the dimeric TcAChE–THA system preparation for the thermodynamic integration simulation included the following steps:

- All missing hydrogen atoms were added, and the system was energy minimized with 200 steps of steepest descent keeping all heavy atoms fixed.
- All close interatomic contacts were identified and relaxed by energy minimization.
- Crystal water molecules were added (82/monomer) and the entire system was solvated with SPC/E water molecules in a rectangular box in such a way that the minimum distance between water oxygen atoms and other heavy atoms was 2.5 Å, and the distance from the box walls to the protein atoms was not smaller than 10 Å.
- All water molecules were energy minimized with 200 steepest descent steps. Those water molecules that entered protein cavities and had repulsive potential energies with solute and other water molecules and could not form at least 2–3 hydrogen bonds were deleted. Energy minimization of the remaining solvent molecules was repeated.
- Three concentric spheres were defined around the hydrogen atom at position 6 in THA (the hydrogen atom that is substituted with chlorine in ClTHA) with radii 20, 30, and 50 Å. All solvent molecules outside the 50 Å sphere were deleted, while those located between 30 and 50 Å were per-

manently fixed. The rest of the water molecules were dynamically equilibrated for 20 ps at 298 K using a cutoff radius of 6 Å for nonbonding interactions.

— All solvent molecules outside the 30 Å sphere were discarded, and only that part of the solute that belongs to the 20 Å sphere was energy minimized and subsequently dynamically equilibrated at 100, 200, and 298 K for 5 ps at each temperature, with atom velocity reassignment each 0.2 ps. The rest of the system was kept frozen. In this part of the equilibration the cutoff radius of 10 Å was used.

— A complete dynamic equilibration (solute + solvent) at 298 K inside the inner sphere of 20 Å was done for 10 ps with a 10 Å cutoff radius and 0.2 ps velocity reassignment.

During the MCTI simulation the dynamic part of the system was limited to the 20 Å inner sphere defined above. $\Delta\lambda$ was kept constant at a value of 0.05, which corresponds to 21 simulation steps. For each λ, the system was equilibrated with 1000 steps of 0.002 ps length, followed by 3000 data gathering steps, where ensemble averages were determined and ΔG accumulated.

Calculation of Electrostatic Binding Energies

The electrostatic part of the binding energies of THA and ClTHA by TcAChE was estimated with Poisson–Boltzmann calculations, where solvent is treated as a polarizable continuum. Assuming that enzyme, inhibitors, and enzyme–inhibitor complexes are described by their predominant conformational and ionization states, the binding free energies ΔG_b were obtained from

$$\Delta G_b = \Delta G_{\mathrm{AChE}-L} - (\Delta G_{\mathrm{AChE}} + \Delta G_L) \qquad (2)$$

where L = THA or ClTHA. The calculations were done with the OPLS[22] atomic parameter set for the protein and ab initio atomic charges for inhibitors. The dielectric constants were set at commonly used values of 78 and 4 for solvent and protein, respectively. Calculations were done at 0 ionic strength. The assumption about the absence of solution ions makes possible direct comparison with the MCTI free energy results obtained at the similar conditions. In order to increase the accuracy of the calculated electrostatic potential, we used a so-called grid focusing method[24]: after initial solution of the Poisson–Boltzmann equation, the calculation was repeated with a finer grid with boundary conditions taken from the previous solution. We have used the following grids: ($70 \times 70 \times 70$) with spacing 2.7 Å and ($90 \times 90 \times 90$) with spacing 1.0 Å.

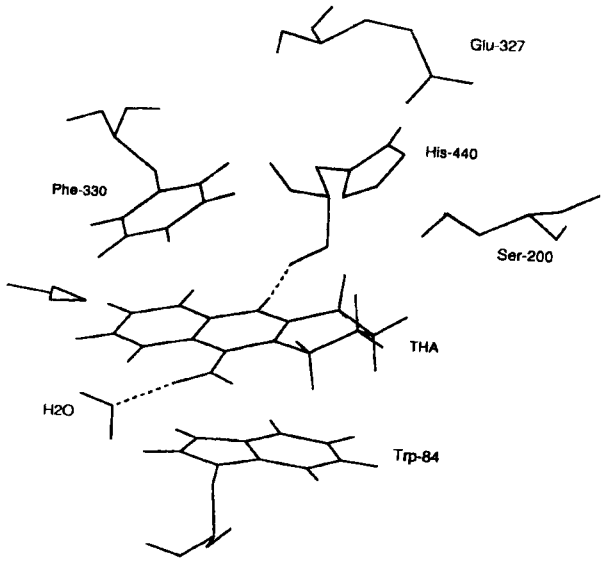

FIGURE 2 Protonated tacrine in the active site of TcAChE. The arrow indicates the hydrogen atom which is substituted with chlorine.

RESULTS AND DISCUSSION

Ligand and TcAChE–THA Complex Structures

Two THA conformations were found with ab initio calculations. They correspond to boat and chair configurations of the 6-membered hydrogenated ring. The latter is 3.6 kcal/mol more stable in vacuum, and is separated from the boat conformation by a barrier of 4.0 kcal/mol for the chair → boat isomerization process. We assume that the same order of stability occurs for ClTHA and for both protonated molecules in solution. Therefore in all simulations we have used the chair conformation. Protonation of THA occurs predominantly on the ring nitrogen atom. Our ab initio calculations predict that the gas-phase stability of the N-ring protonated THA molecule is 40.4 kcal/mol greater than the N-amino protonated one, which implies that the population of the latter should be close to zero at room temperature. This prediction is in agreement with titration calculation results given below. In the ring protonated form, the amino group becomes planar due to electron redistribution upon protonation, an effect that might be expected qualitatively by the consideration of resonance structures for that isomer. CHELPG atomic charges for neutral and protonated THA and ClTHA molecules are given in the Appendix.

Figure 2 shows the position of the THA mole-

Table I Average Charges and Two Lowest Energy Ionization States in the TcAChE–THA Complex at pH 7 and 85 m*M* Ionic Strength[a]

Residue	Average Charge	Ionization State A	Ionization State B
Asp-392	−0.39	0	0
His-440	0.49	1	0
Glu-443	−0.72	−1	0
His-471	0.81	1	1

[a] Only residues that deviate significantly in their mean charges from the standard values are listed.

cule in the active site of TcAChE enzyme taken from the model structure obtained as described in Methods. At pH 7, THA is protonated (see below) and forms two hydrogen bonds: one between the ring nitrogen and the main-chain carbonyl oxygen of His-440, and another one between the amino group nitrogen and the oxygen from crystal water 32. A part of the THA binding potential energy must come from its interaction with aromatic side chains of Trp-84 and Phe-330, because, as Figure 2 shows, THA is positioned between them. During a 20 ps molecular dynamics run (preceded with the equilibration protocol described in the section on thermodynamic integration) the structure shown in Figure 2 was retained.

Ionization States of the TcAChE–THA Complex

The calculated mean charge of the monomeric TcAChE complex at pH 7 and ionic strength of 85 m*M* is $-6.3e$. As anticipated from the quantum chemical calculations of THA, the average charge of $+1e$ is located on the ring nitrogen. Assuming that standard charges for all Lys and Arg residues are +1, for Glu and Asp −1, and for His 0, most of the ionizable groups in the TcAChE–THA complex have their mean charges close to the standard values except for four residues listed in Table I. Table I also shows the two lowest energy ionization states of the TcAChE–THA complex, which differ only in the charge of the His-440 and Glu-443 residues. The energy gap between them is only 0.14 kcal/mol, with the preference of charged His-440 and Glu-443 (state B in Table I), but taking into account the approximate nature of the model we have to assume that both states are equally probable and have to be considered in the analysis of THA binding. The charge of His-440 and Glu-443 might be critical for THA binding, because, as the crystal structure reveals, THA is positioned in close proximity to both of those residues, particularly His-440. It is interesting that when THA is removed from the enzyme, the calculated pKa of His-440 increases by 3 units. We address the significance of that behavior elsewhere.[25] Here we mention only that THA is not unique in that behavior and that any positive ion placed in the active site of TcAChE enables deprotonation of His-440, which is crucial for catalytic action.

Binding Energies

Figure 3 shows the variations of calculated ΔG with perturbation parameter λ for processes 3 and 4. The striking feature of the results shown in Figure 3 is that only the ionization state B of the TcAChE shows stronger binding of ClTHA relative to that of THA. Table II contains calculated ΔG_3, ΔG_4, and $\Delta\Delta G = \Delta G_4 - \Delta G_3$ values. It also contains binding energies ΔG_1 and ΔG_2 determined with PB calculations described in Electrostatic Binding Energy Calculations. It is clearly visible that state A of the protein is unlikely to bind either inhibitor, due to electrostatic effects. The most likely reason is that positively charged His-440 destabilizes the TcAChE–THA and TcAChE–ClTHA complexes by electrostatic repulsion with the cationic inhibitor. Charged Glu-443 is apparently too far to compensate for that energetically unfavorable effect.

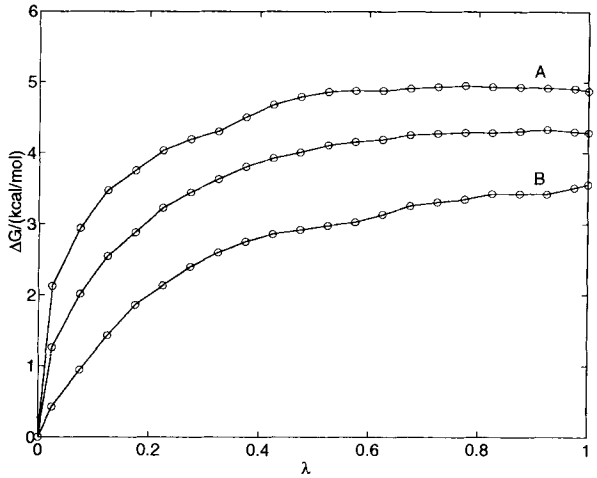

FIGURE 3 Calculated ΔG as a function of perturbation parameter λ coupling tacrine and 6-chlorotacrine inside the active site of TcAChE and in water (middle curve). Curves A and B refer to two ionization states of the protein (see text).

Table II MCTI and Electrostatic PB Calculation Results for the ΔG Values for Processes 1–4 Shown in Figure 1[a]

	ΔG_1		ΔG_2		ΔG_3	ΔG_4		$\Delta\Delta G$	
Technique	A	B	A	B		A	B	A	B
MCTI					4.28 ± 0.27	4.87 ± 0.45	3.56 ± 0.33	0.6 ± 0.5	-0.7 ± 0.4
PB[b]	2.08 ± 0.14	-2.86 ± 0.12	1.78 ± 0.16	-3.29 ± 0.19				-0.30 ± 0.21	-0.43 ± 0.22
Experiment								-0.7 ± 0.11[c]	
								-1.7 ± 0.16[d]	

[a] Last column contains the free energy differences $\Delta\Delta G = \Delta G_2 - \Delta G_1 = \Delta G_4 - \Delta G_3$. Experimental $\Delta\Delta G$ values are determined from $\Delta\Delta G = RT \ln(IC_{50}^{ClTHA}/IC_{50}^{THA})$, where R is the gas constant, T is the temperature, and IC_{50}^{ClTHA} and IC_{50}^{THA} are measured IC_{50} factors for THA and ClTHA inhibitors taken from Ref. 5. A and B refer to two protein ionization states (see text). All free energies are in kcal/mol.

[b] Average ΔG values from 5 PB runs with slightly displaced grid origin (≤ 0.5 Å). Error bars represent standard deviations.

[c] Electric eel AChE.

[d] Human red blood cells AChE.

Table II also shows a fairly good agreement between the $\Delta\Delta G$ values derived from MCTI and PB calculations. In Table II we include also the $\Delta\Delta G$'s for processes 1 and 2 determined from the experimental IC_{50} values for electric eel and human red blood cell AChE. The experimental $\Delta\Delta G$'s are derived from the competitive inhibition equation:

$$IC_{50} = K_i\left(1 + \frac{[S]}{K_m}\right) \tag{3}$$

and the fact that the substrate concentration $[S]$ was the same for both inhibitors. K_m and K_i are Michaelis and enzyme-inhibitor dissociation constants, respectively. It can be seen that experimental data for electric eel AChE inhibition are in excellent agreement with our MCTI results for TcAChE. This agreement might be a bit fortuitous because one cannot expect ideal agreement between data obtained for an enzyme produced by two different organisms, even when the enzymes are highly homologous. The important result is, however, that two different computational techniques both predict stronger binding of ClTHA with respect to the parent THA molecule.

Separate PB calculations of the hydration energies for the inhibitor molecules show that the protonated ClTHA is hydrated stronger than THA by 0.3 kcal/mol (the respective values are 44.3 and 44.0 kcal/mol). This result indicates that solubility in water is not likely to drive the binding of THA and ClTHA by TcAChE. In fact, the interaction between ClTHA and TcAChE has to be strong enough to compensate for the hydration effects that favor the formation of the TcAChE–THA complex relative to the TcAChE–ClTHA one.

From the PB binding data, one may conclude that the stronger binding of ClTHA is due largely to the electrostatic part of the interaction potential. As mentioned above, the THA molecule is positioned between two aromatic groups, which implies that at least a part of the attractive potential between ligand and protein may come from the interaction of the π electrons of Phe-330 and Trp-84 with the delocalized positive charge of the ligand. According to recent quantum chemical calculations of Kim et al.,[26] the nature of that interaction is mainly attraction of the quadrupole and induced dipole moments of the aromatic system with the positive charge of the ion. Although the potential function used in the MCTI calculations does not describe the polarization interaction at all, the first mentioned component is approximated by the use

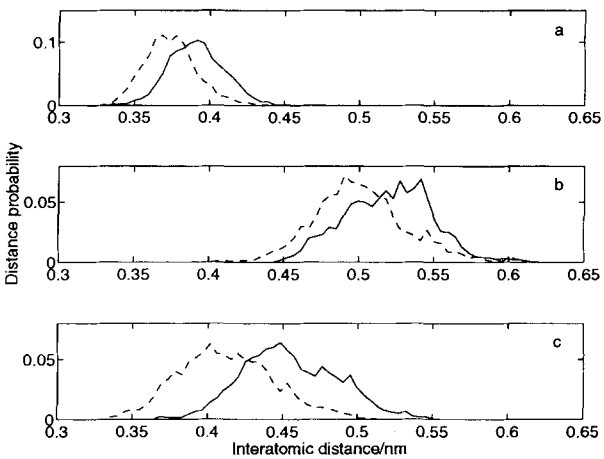

FIGURE 4 Distance histograms for the following THA/ClTHA and enzyme atoms: (a) C4-CG(Trp-84), (b) C5-CZ2(Trp-84), and (c) N1-CZ(Phe-330). Inhibitor atom numbers are shown in Scheme II. Distances were recorded every step of 20 ps in the MD simulations of the TcAChE–THA (solid lines) and TcAChE–ClTHA (broken lines) systems.

of partial atomic charges on aromatic carbon and hydrogen atoms. Molecular dynamics (MD) runs of TcAChE–THA and TcAChE–ClTHA, in their ionization states B, reveal that the average distances between the Phe-330 and Trp-84 side chains and ligand atoms are shorter for ClTHA than THA. This is illustrated in Figure 4, which shows three distance histograms for the studied systems. The possible explanation of the enhanced attractive interaction caused by chlorine substitution of the ligand is the more favorable charge distribution on the aromatic rings of THA molecule. If this interpretation is correct, we can expect that other, more polar substituents than chlorine atom could enhance even further the inhibitory effect of the corresponding substituted tacrine. It might be noticed here that qualitatively the same conclusion regarding the THA and ClTHA interactions with two adjacent aromatic residues could perhaps be obtained by the simulation of a model system containing Phe-330, Trp-84, and inhibitor only. The analysis of isolated fragments of drug–receptor systems can sometimes provide useful insights to the physics of binding. Ultimately however, more comprehensive models are to be desired to account for the actual environment in which the interaction occurs in order to obtain reliable quantitative results. Part of the significance of this work is to take a step toward such comprehensive models by combining Poisson–Boltzmann and molecular dynamics/thermodynamic integration methods, which have separately proven to provide reliable results for protein titration phenomena and free energy changes in comparison with the experiment.

Because of tacrine location between the two aromatic groups, we might expect that another factor contributing to its binding is charge transfer interaction resulting from delocalization of Trp-84 and Phe-330 π electrons into tacrine orbitals. The importance of this interaction for binding of *N*-methylacridinium by AChE was demonstrated experimentally by Shinitzky et al. more than two decades ago.[27] This type of interaction is not explicitly taken into account in our simulations, but we might expect that chlorotacrine is a better electron acceptor than the unsubstituted parent molecule, and that the usage of inhibitor vacuum atomic charges at least partly accounts for the stabilization energy caused by charge transfer.

CONCLUSIONS

The following conclusions can be derived from the current study:

1. The calculations described in the present study of the AChE inhibition by tacrine and chlorotacrine are in agreement with experimental observations. Thermodynamic integration simulation predicts that substitution of hydrogen by chlorine at position 6 in THA leads to an increase of the inhibitor binding strength by 0.7 ± 0.4 kcal/mol. Similar stabilization by 0.43 ± 0.22 kcal/mol is predicted by electrostatic Poisson–Boltzmann calculations indicating that electrostatic effects mostly contribute to the differences in binding between the two inhibitors.

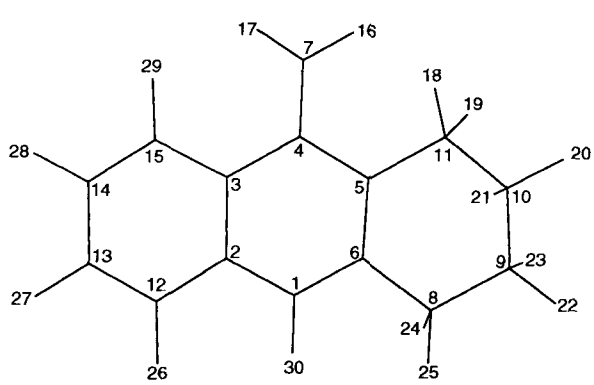

SCHEME II

Table III Atomic Charges and Radii for the THA and ClTHA Inhibitors

Atom	Atomic Charges (e)				Atomic Radii (Å)
	THA	$(THA)H^+$	ClTHA	$(ClTHA)H^+$	
N1	−0.76	−0.72	−0.73	−0.69	1.625
C2	0.55	0.53	0.49	0.48	1.775
C3	−0.23	−0.28	−0.23	−0.26	1.775
C4	0.47	0.66	0.48	0.65	1.750
C5	−0.48	−0.43	−0.47	−0.42	1.875
C6	0.51	0.45	0.51	0.45	1.875
N7	−0.86	−0.93	−0.87	−0.93	1.625
C8	−0.07	−0.05	−0.11	−0.10	1.953
C9	0.08	0.07	0.12	0.10	1.953
C10	−0.01	0.01	−0.06	−0.07	1.953
C11	0.27	0.16	0.28	0.18	1.953
C12	−0.27	−0.37	−0.24	−0.32	1.775
C13	−0.05	0.08	0.16	0.21	1.775
C14	−0.19	−0.19	−0.19	−0.16	1.775
C15	−0.07	−0.01	−0.09	−0.03	1.775
H16	0.36	0.44	0.37	0.44	1.200
H17	0.36	0.45	0.37	0.45	1.200
H18	−0.03	0.00	−0.03	0.00	0.000
H19	−0.05	0.00	−0.05	0.00	0.000
H20	−0.01	0.00	0.00	0.02	0.000
H21	−0.02	0.02	0.01	0.04	0.000
H22	−0.03	−0.01	−0.03	−0.01	0.000
H23	−0.01	0.02	−0.02	0.02	0.000
H24	0.03	0.04	0.04	0.05	0.000
H25	0.04	0.05	0.05	0.06	0.000
H26	0.14	0.18	0.15	0.17	1.210
H27/Cl27	0.11	0.13	−0.16	−0.06	1.210/1.900
H28	0.12	0.16	0.13	0.16	1.210
H29	0.10	0.11	0.12	0.13	1.210
H30		0.43		0.44	1.210

2. Molecular dynamics simulation demonstrates that the average distances between Phe-330 and Trp-84 side chains and ClTHA aromatic rings are shorter than in the case of unsubstituted THA, which suggests that electrostatic interaction between protein π electrons and the inhibitor cation is partly responsible for the observed inhibition differences. Reduced electron density on tacrine aromatic rings upon chlorination could be a reason for the stronger attraction between ClTHA and adjacent side groups of Phe-330 and Trp-84. We expect therefore that substituents with higher electron withdrawing properties might provide even stronger inhibition of AChE.
3. Our combined MCTI/MD/PB computational study demonstrated the critical role of the ionization state of AChE on THA and ClTHA binding: the calculations suggest strongly that only the ionization state in which His-440 is deprotonated can bind both inhibitors. This emphasizes the necessity of careful analysis of the protein ionization states for the proper description of the model system that is used for molecular dynamics simulation.

APPENDIX

In Scheme II and Table III we provide atomic charges for THA and ClTHA molecules used in the current study.

We thank Prof. Palmer Taylor for helpful discussions. This work has been supported in part by grants from

This work has been supported in part by grants from NSF, NIH, and the MetaCenter Program of the NSF Supercomputer Centers. We would also like to thank Biosym Technologies for its support. Pacific Northwest Laboratories are operated by Battelle Memorial Institute for the U.S. Department of Energy.

REFERENCES

1. Giacobini, E., (1995) in *Enzymes of the Cholinesterase Family,* Balasubramanian, A. S., Doctor, B. P., Taylor, P. & Quinn, D. M., Eds., Plenum Press, New York, in press.
2. Enz, A. (1993) *Prog. Brain Res.* **98,** 431–438.
3. Mooser, G. & Sigman, D. (1972) *Biochemistry* **13,** 2299–2305.
4. Radić, Z., Pickering, N. A., Vellom, D. C., Camp, S. & Taylor, P. (1993) *Biochemistry* **32,** 12074–12084.
5. Gregor, V. E., Emmerling, M. R., Lee, C. & Moore, C. J. (1992) *Med. Chem. Lett.* **2,** 861–864.
6. Straatsma, T. P. & McCammon, J. A. (1991) *J. Chem. Phys.* **95,** 1175–1188.
7. Madura, J. D., Davis, M. E., Gilson, M. K., Wade, R. C., Luty, B. A. & McCammon, J. A. (1994) *Rev. Comp. Chem.* **5,** 229–267.
8. Harel, M., Schalk, I., Ehret-Sabatier, L., Bouet, F., Goeldner, M., Hirth, C., Axelsen, P., Silman, I. & Sussman, J. L. (1993) *Proc. Natl. Acad. Sci. USA* **90,** 9031–9035.
9. Pop, E., Brewster, M. E., Kaminski, J. J. & Bodor, N. (1989) *Int. J. Quant. Chem.* **35,** 315–324.
10. Frisch, M. J., Trucks, G. W., Head-Gordon, M., Gill, Wong, M. W., Foresman, J. B., Johnson, B. G., Schlegel, H. B., Robb, M. A., Replogle, E. S., Gomperts, R., Andres, J. L., Raghavachari, K., Binkley, J. S., Gonzalez, C., Martin, R. L., Fox, D. J., Defrees, D. J., Baker, J., Stewart, J. J. P. & Pople, J. A. (1992) *Gaussian 92,* Revision E.2, Pittsburgh, PA.
11. Breneman, C. M. & Wiberg, K. B. (1990) *J. Comput. Chem.* **11,** 361–373.
12. Antosiewicz, J., McCammon, J. A. & Gilson, M. K. (1994) *J. Mol. Biol.* **238,** 415–436.
13. Davis, M. E., Madura, J. D., Luty, B. A. & McCammon, J. A. (1991) *Comput. Phys. Commun.* **62,** 187–197.
14. Antosiewicz, J. & Porschke, D. (1995) *Biophys. J.* **68,** 655–664.
15. Gilson, M. K. (1993) *Proteins* **15,** 266–282.
16. Brooks, B. R., Bruccoleri, R. E., Olafson, R. E., States, B. D., Swaminathan, D. J. & Karplus, M. (1982) *J. Comput. Chem.* **4,** 187–217.
17. Jorgensen, W. L. & Tirado-Rives, J. (1988) *J. Am. Chem. Soc.* **110,** 1657–1666.
18. Gilson, M. K., Straatsma, T. P., McCammon, J. A., Ripoll, D. R., Faerman, C. H., Axelsen, P. H., Silman & Sussman, J. L. (1994) *Science* **263,** 1276–1278.
19. Antosiewicz, J., Gilson, M. K. & McCammon, J. A. (1994) *Isr. J. Chem.* **34,** 151–158.
20. Straatsma, T. P. & McCammon, J. A. (1990) *J. Comput. Chem.* **11,** 943–951.
21. Weiner, S. J., Collman, P. A., Case, D. A., Singh, U. C., Ghio, C., Alagona, G., Profeta, S. J. & Weiner, P. J. (1984) *J. Am. Chem. Soc.* **106,** 765–784.
22. Weiner, S. J., Kollman, P. A., Nguyen, D. T. & Case, D. A. (1986) *J. Comput. Chem.* **7,** 230–252.
23. Smith, P. E., Dang, L. X. & Pettitt, B. M. (1991) *J. Am. Chem. Soc.* **113,** 67–73.
24. Gilson, M. K., Sharp, K. A. & Honig, B. H. (1988) *J. Comput. Chem.* **9,** 327–335.
25. Wlodek, S., Antosiewicz, J., McCammon, J. A. & Gilson, M. K. (1995) in *Modeling of Biomolecular Structures and Mechanisms,* Pullman, A., Jortner, J. & Pullman, B., Eds., Kluwer Academic Publishers, pp. 25–37.
26. Kim, K. S., Lee, J. Y., Lee, S. J., Ha, T. K. & Kim, D. H. (1994) *J. Am. Chem. Soc.* **116,** 7399–7400.
27. Shinitzky, M., Dudai, Y. & Silman, I. (1973) *FEBS Lett.* **30,** 125–128.